

## Soret And Dufour Effects On Mhd Boundary Layer Flow Of A Chemically Reacting Fluid Past A Moving Vertical Plate With Viscous Dissipation

E. Manjoolatha<sup>1\*</sup>, A. Neeraja<sup>2</sup>, M. Prasannalakshmi<sup>3</sup>, and N. Bhaskar Reddy<sup>4</sup>

<sup>1</sup>. Dept. of Mathematics, Annamacharya Inst. of Tech & Science, Tirupati, AP, India

<sup>2</sup>. Dept. of Mathematics, Aditya College of Engineering, Surampalem, AP, India

<sup>3</sup>. Dept. of Mathematics, Sree Vignana Deepthi Degree College, Chittoor, AP, India

<sup>4</sup>. Dept. of Mathematics, Sri Venkateswara University, Tirupati, AP, India

Corresponding author: E. Manjoolatha

### ABSTRACT

The object of the present paper is to investigate the Soret and Dufour effects on a steady free convection boundary layer flow of a viscous, incompressible electrically conducting and chemically reacting fluid past a low-heat-resistant sheet moving vertically downwards, by taking viscous dissipation into account. The governing equations are transformed into a set of ordinary differential equations by using similarity transformation and the resultant equations are solved numerically using the fourth order Runge-Kutta method along with shooting technique. The effects of various governing parameters on the velocity, temperature, concentration, skin-friction coefficient, Nusselt number and Sherwood number are shown in figures and tables and discussed in detail.

**Key words:** Boundary layer flow, Chemical reaction, Soret and Dufour effects, Viscous Dissipation, Vertical plate.

Date of Submission: 25-08-2017

Date of acceptance: 13-09-2017

### I. INTRODUCTION

Boundary layers formed across vertical surfaces are a common engineering problem in industry. Some practical areas of application include chemical coating of flat plates, hot rolling, wire drawing, metal and polymer extrusion processes. Many chemical engineering processes like metallurgical and polymer extrusion involve cooling of molten liquid. Some polymer fluids like Polyethylene oxide and polyisobutylene solution in cetane have better electromagnetic properties and can be regulated by external magnetic fields. A comprehensive review on the subject has been made by many authors including Nield and Bejan [1], Ingham and Pop [2,3], Bejan and Khair [4], Trevisan and Bejan [5] and Sakiadis [6]. Postelnicu [7] numerically studied the influence of magnetic field on heat and mass transfer by natural convection from vertical surfaces in porous media by considering the Soret and Dufour effects while Anghel et al. [8] analyzed the Dufour and Soret effects on free convection boundary layer over a vertical surface embedded in a porous medium. Furthermore, Alam and Rahman [9] also investigated the Dufour and Soret effects on mixed convection flow past a vertical porous flat plate

with variable suction. Free convection on a vertical plate with uniform and constant heat flux in a thermally stratified micropolar fluid was presented by Chang and Lee [10] whilst Vajravelu et al. [11] and Crane [12] investigated the convective heat transfer on a stretching sheet. Also, Gupta and Gupta [13], Kays and Crawford [14], Ibrahim and Makinde [15,16] made significant contributions to the subject by considering various aspects of the problem of heat and mass transfer on stretching sheets.

Anwar et al. [17] conducted a network numerical study on laminar free convection flow from a continuously-moving vertical surface in thermally-stratified non-Darcian high-porosity medium. Makinde [18] earlier on presented computational results on boundary layer flow with heat and mass transfer past a moving vertical porous plate. The effect of thermal radiation on heat and mass transfer of a variable viscosity fluid past a vertical porous plate permeated by transverse magnetic field was reported in Makinde and Ogulu [19].

In all the above papers viscous dissipation is neglected. But when the motion is under strong gravitational field, or flow field is of extreme size, the viscous dissipative heat cannot be neglected.

Gebhart [20] has shown the importance of viscous dissipative heat in free convection flow in the case of isothermal and constant heat flux at the plate. Gebhart and Mollendorf [21] considered the effects of viscous dissipation for external natural convection flow over a surface. Soundalgekar [22] analyzed viscous dissipative heat on the two-dimensional unsteady free convective flow past an infinite vertical porous plate. Isreal-Cookey et al. [23] investigated the influence of viscous dissipation and radiation on unsteady MHD free convection flow past an infinite heated vertical plate in a porous medium with time dependent suction. Soundalgekar et al. [24] studied the finite difference analysis of mass transfer effects on flow past an impulsively started infinite isothermal vertical plate in a dissipative fluid.

In view of the above observations, an attempt is made to study the Soret and Dufour effects on a steady free convection boundary layer flow of a viscous, incompressible electrically conducting and chemically reacting fluid past a low-heat-resistant sheet moving vertically downwards, by taking viscous dissipation into account.

## II. MATHEMATICAL ANALYSIS

A steady two-dimensional laminar free convection flow of a viscous incompressible electrically conducting and chemically reacting fluid along a semi-infinite vertically moving flat plate is considered, by taking Soret and Dufour effects and viscous dissipation into account. The x-axis is taken along the plate in the upward direction and the y-axis is taken normal to it. A uniform magnetic field is applied in the direction perpendicular to the plate. The transverse applied magnetic field and magnetic Reynolds number are assumed to be very small, so that the induced magnetic field and Hall effects are negligible. All the fluid properties are assumed to be constant except that the influence of density variation with temperature in the body force term (Boussinesq's approximation). Now, under the above assumptions, the governing boundary layer equations of the flow field are

Continuity equation

$$\frac{\partial u}{\partial x} + \frac{\partial v}{\partial y} = 0 \quad (1)$$

Momentum equation

$$u \frac{\partial u}{\partial x} + v \frac{\partial u}{\partial y} = \nu \frac{\partial^2 u}{\partial y^2} - \frac{\sigma H_0^2}{\rho} u + g \beta_T (T - T_\infty) + g \beta_c (C - C_\infty) \quad (2)$$

Energy equation

$$u \frac{\partial T}{\partial x} + v \frac{\partial T}{\partial y} = \alpha \frac{\partial^2 T}{\partial y^2} + \frac{D_m k_T}{c_s c_p} \frac{\partial^2 C}{\partial y^2} + \frac{\sigma H_0^2}{\rho c_p} u^2 + \frac{\nu}{\rho c_p} \left( \frac{\partial u}{\partial y} \right)^2$$

(3)

Species equation

$$u \frac{\partial C}{\partial x} + v \frac{\partial C}{\partial y} = D \frac{\partial^2 C}{\partial y^2} + \frac{D_m k_T}{T_m} \frac{\partial^2 T}{\partial y^2} - \gamma (C - C_\infty)$$

(4)

The boundary conditions for the velocity, temperature and concentration fields are

$$u = Bx, v = 0, T = T_w = ax + T_\infty, C = C_w = bx + C_\infty \quad \text{at } y = 0$$

$$u \rightarrow 0, T \rightarrow T_\infty, C \rightarrow C_\infty \quad \text{as } y \rightarrow \infty$$

(5)

where respectively,  $u$  and  $v$  are the velocity components in the  $x$  and  $y$  directions,  $T$  and  $C$  are the fluid temperature and concentration,  $T_w$  and  $C_w$  are the wall surface temperature and concentration,  $T_\infty$  and  $C_\infty$  are the fluid temperature and concentration at a distant location from the surface,  $\beta$  is the thermal expansion coefficient,  $\nu$  is the kinematic viscosity,  $\alpha$  is the thermal diffusivity,  $D$  is the mass diffusivity,  $a$  and  $b$  are constants.

Generally, we consider the case where the surface temperature and concentration  $T_w(x)$  and  $C_w(x)$  are greater than the ambient temperature  $T_\infty$  and concentration  $C_\infty$ . Under these conditions, the free convective motion of the fluid is upward along the plate. In a reverse scenario, where the surface is colder than the ambient temperature and concentration,  $T_w(x) < T_\infty$  and  $C_w(x) < C_\infty$ , the boundary layer profile remains the same but the direction is reversed, i.e. the fluid flow is downward.

To transform equations (2)-(4) into a set of ordinary differential equations, the following similarity transformations and dimensionless variables are introduced.

$$\eta = y \sqrt{\frac{B}{\nu}}, \quad \psi = x \sqrt{\nu B} f(\eta),$$

$$\theta(\eta) = \frac{T - T_\infty}{T_w - T_\infty}, \quad \phi(\eta) = \frac{C - C_\infty}{C_w - C_\infty},$$

$$Ha = \frac{\sigma H_0^2}{\rho B}, \quad Pr = \frac{\nu}{\alpha}, \quad Gr = \frac{g \beta_T (T_w - T_\infty)}{xB^2},$$

$$Gc = \frac{g \beta_c (C_w - C_\infty)}{xB^2},$$

$$Du = \frac{D_m k_T (C_w - C_\infty)}{c_s c_p (T_w - T_\infty)},$$

$$Sr = \frac{D_m k_T (T_w - T_\infty)}{\nu T_m (C_w - C_\infty)}, Ec = \frac{x^2 B^2}{c_p (T_w - T_\infty)}.$$

(6)

where  $\eta$  - the dimensionless variable,  $\psi$  - the stream function,  $\theta$  - the dimensionless temperature,  $\phi$  - the dimensionless concentration,  $Ha$  - the Hartmann number,  $Pr$  - the Prandtl number,  $Gr$  - the local thermal Grashof number,  $Gc$  - the local solutal Grashof number,  $Du$  - the Dufour number,  $Sr$  - the Soret number and  $Ec$  - the Eckert number. The mass concentration equation (1) is satisfied by the Cauchy-Riemann equations

$$u = \frac{\partial \psi}{\partial y} \quad \text{and} \quad v = -\frac{\partial \psi}{\partial x}$$

(7)

In view of equations (6)-(7), equations (2) to (4) transform into

$$f''' + ff'' - f'^2 - Haf' + Gr\theta + Gc\phi = 0$$

(8)

$$\theta'' + Pr f\theta' - Pr\theta f' - Ha Pr Ec f'^2 + Pr Ec f''^2 + Pr Du \phi'' = 0$$

(9)

$$\phi'' + Sc f\phi' - Sc\phi f' - Sc\beta\phi + Sc Sr\theta'' = 0$$

(10)

The corresponding boundary conditions are

$$f' = 1, f = 0, \theta = 1, \phi = 1 \quad \text{at} \quad \eta = 0$$

$$f' = 0, \theta = 0, \phi = 0 \quad \text{as} \quad \eta \rightarrow \infty$$

(11)

where the primes indicate differentiation with respect to  $\eta$ .

Other physical quantities of interest in the problems of this type are the skin friction

parameter  $C_f = 2(Re)^{-\frac{1}{2}} f''(0)$ , the plate surface temperature  $\theta(0)$ , Nusselt number

$Nu = -(Re)^{\frac{1}{2}} \theta'(0)$  and the Sherwood number

$Sh = -(Re)^{\frac{1}{2}} \phi'(0)$  (where  $Re = \frac{U_t}{\nu}$  is the

Reynolds number). For local similarity case, integration over the entire plate is necessary to obtain the total skin friction, total heat and mass transfer rates.

### III. SOLUTION OF THE PROBLEM

The set of coupled non-linear governing boundary layer equations (7)-(9) together with the boundary conditions (10) are solved numerically by

using Runge-Kutta fourth order technique along with shooting method. First of all, higher order non-linear differential Equations (7)-(9) are converted into simultaneous linear differential equations of first order and they are further transformed into initial value problem by applying the shooting technique (Jain *et al.*[7]). The resultant initial value problem is solved by employing Runge-Kutta fourth order technique. The step size  $\Delta \eta = 0.05$  is used to obtain the numerical solution with five decimal place accuracy as the criterion of convergence. From the process of numerical computation, the skin-friction coefficient, the Nusselt number and the Sherwood number, which are respectively proportional to  $f''(0)$ ,  $-\theta'(0)$  and  $-\phi'(0)$ , are also sorted out and their numerical values are presented in a tabular form.

### IV. RESULTS AND DISCUSSION

The governing equations (7)-(9) subject to the boundary conditions (10) are integrated as described in section 3. The Prandtl number is taken to be  $Pr=0.71$  which corresponds to air, the value of Schmidt number ( $Sc$ ) were chosen to be  $Sc=0.24, 0.62, 0.78, 2.62$ , representing diffusing chemical species of most common interest in air like  $H_2$ ,  $H_2O$ ,  $NH_3$  and Propyl Benzene respectively. The effects of various parameters on the velocity in the boundary layer are depicted in Figs. 1-9. The effects of various parameters on the temperature in the boundary layer are depicted in Figs. 10-17. The effects of various parameters on the concentration in the boundary layer are depicted in Figs. 18-25.

Fig. 1 depicts the effect of magnetic parameter ( $Ha$ ) strength on the momentum boundary layer thickness. It is now a well established fact that the magnetic field presents a damping effect on the velocity field by creating drag force that opposes the fluid motion, causing the velocity to decrease. However, in this case an increase in the  $Ha$  only slightly slows down the motion of the fluid away from the vertical plate towards the free stream velocity, while the fluid velocity near the vertical plate increases. Fig.2 illustrates the effect of the thermal Grashof number ( $Gr$ ) on the velocity field. The thermal Grashof number signifies the relative effect of the thermal buoyancy force to the viscous hydrodynamic force. The flow is accelerated due to the enhancement in buoyancy force corresponding to an increase in the thermal Grashof number i.e. free convection effects. It is noticed that the thermal Grashof number ( $Gr$ ) influences the velocity within the boundary layer when compared to far away from

the plate. It is seen that as the thermal Grashof number ( $Gr$ ) increases, the velocity increases.

The effect of solutal Grashof number ( $Gc$ ) on the velocity is illustrated in Fig.3. The solutal Grashof number ( $Gc$ ) defines the ratio of the species buoyancy force to the viscous hydrodynamic force. It is noticed that the velocity increases with increasing values of the solutal Grashof number. Further as the solutal Grashof number ( $Gc$ ) increases, the velocity field near the boundary layer increases. It is noticed that, for higher values of solutal Grashof number ( $Gc$ ), the profiles are found to be more parabolic. Fig.4 illustrates the effect of Prandtl number ( $Pr$ ) on the velocity. It is noticed that as the Prandtl number ( $Pr$ ) increases, the velocity decreases. As seen in the earlier cases, far away from the plate, the effect is not that much significant.

Fig.5 illustrates the effect of the Schmidt number ( $Sc$ ) on the velocity. The Schmidt number ( $Sc$ ) embodies the ratio of the momentum diffusivity to the mass (species) diffusivity. It physically relates the relative thickness of the hydrodynamic boundary layer and mass-transfer (concentration) boundary layer. It is observed that as Schmidt number ( $Sc$ ) increases the velocity decreases. Fig. 6 shows the variation of the velocity boundary-layer with the Eckert number ( $Ec$ ). It is noticed that the velocity boundary layer thickness decreases with an increase in the Eckert number. Fig. 7 shows the variation of the velocity boundary-layer with the chemical reaction rate constant ( $\beta$ ). It is found that the velocity boundary layer thickness decreases with an increase in the chemical reaction rate constant. Fig. 8 shows the variation of the velocity boundary-layer with the Dufour number ( $Du$ ). It is noticed that the velocity boundary layer thickness increases with an increase in the Dufour number. Fig. 9 depicts the variation of the velocity boundary-layer with the Soret number ( $Sr$ ). It is noticed that the velocity boundary layer thickness increases with an increase in the Soret number.

The effect of the magnetic parameter ( $Ha$ ) on the temperature is illustrated in Fig.10. It is observed that as the magnetic parameter increases, the temperature decreases. From Figs. 11 and 12, it is observed that the thermal boundary layer thickness decreases with an increase in thermal or Solutal Grashof number ( $Gr$  or  $Gc$ ). Fig. 13 illustrates the effect of Prandtl number ( $Pr$ ) on the temperature. It is noticed that as the Prandtl number ( $Pr$ ) increases a decreasing trend in the temperature field is noticed.

Fig.14 illustrates the effect of the Eckert number ( $Ec$ ) on the temperature. It is noticed that as the Eckert number increases, the temperature decreases. Fig. 15 shows the variation of the thermal boundary-layer with the chemical reaction

rate constant ( $\beta$ ). It is observed that the thermal boundary layer thickness increases with an increase in the chemical reaction rate constant. Fig. 16 shows the variation of the thermal boundary-layer with the Dufour number ( $Du$ ). It is seen that the thermal boundary layer thickness increases with an increase in the Dufour number. Fig. 17 shows the variation of the thermal boundary-layer with the Soret number ( $Sr$ ). It is observed that the thermal boundary layer thickness decreases with an increase in the Soret number.

The effect of magnetic parameter ( $Ha$ ) on the concentration field is illustrated Fig.18. As the magnetic parameter increases the concentration is found to be increasing. The effect of buoyancy parameters ( $Gr, Gc$ ) on the concentration field is illustrated in Figs. 19 and 20. It is noticed that the concentration boundary layer thickness decreases with an increase in the thermal or Solutal Grashof numbers ( $Gr$  or  $Gc$ ). Fig. 21 illustrates the effect of Prandtl number ( $Pr$ ) on the concentration. As the Prandtl number increases, an increasing trend in the concentration field is noticed. The effect of Schmidt number ( $Sc$ ) on the concentration is illustrated in Fig.22. As expected, as the Schmidt number ( $Sc$ ) increases, the concentration decreases. The influence of the chemical reaction rate constant ( $\beta$ ) on the concentration field is shown in Fig.23. It is noticed that the concentration decreases monotonically with the increase of the chemical reaction rate constant. Fig. 24 shows the variation of the concentration boundary-layer with the Dufour number ( $Du$ ). It is observed that the concentration boundary layer thickness decreases with an increase in the Dufour number. Fig. 25 shows the variation of the concentration boundary-layer with the Soret number ( $Sr$ ). It is seen that the concentration boundary layer thickness increases with an increase in the Soret number ( $Sr$ ).

In order to benchmark our numerical results, the present results for the skin -friction, Nusselt number and Sherwood number in the absence of Soret and Dufour numbers, are compared with those of Ibrahim and Makinde[9] and found them in excellent agreement as demonstrated in Table 1. From Table 1, it is evident that the local skin friction together with the local heat and mass transfer rate at the plate increases with increasing intensity of Grashof numbers ( $Gr$  or  $Gc$ ). An increase in the magnetic parameter ( $Ha$ ) causes a decrease in both the skin friction and Sherwood number and a decrease in the surface heat transfer rate. An increase in the Prandtl number ( $Pr$ ) causes a decrease in both the skin friction and Sherwood number and an increase in the surface heat transfer rate. An increase in the Eckert number ( $Ec$ ) causes a decrease in both the skin friction and Sherwood number and an increase

in the surface heat transfer rate. An increase in the chemical reaction rate constant ( $\beta$ ) causes an increase in both the skin friction and heat transfer rate and a decrease in the surface mass transfer rate. Table 2 shows the effects of the Soret and Dufour numbers on the skin-friction coefficient, Nusselt number and the Sherwood number. It is evident that an increase in the Dufour number ( $Du$ ) causes an increase in both the skin friction and Sherwood number and a decrease in the surface heat transfer rate. However, an increase in the Soret number ( $Sr$ ) causes an increase in both the skin friction and surface heat transfer rate and a decrease in the surface mass transfer rate.

## V. CONCLUSIONS

From the numerical results, it is observed that the velocity decreases while the temperature and concentration profiles increase with an increase in the magnetic parameter. An increase in the buoyancy force

parameters, accelerates the fluid velocity but decelerates the temperature due to convective cooling. Further, an increase in the Eckert number causes a decrease in both the skin friction and Sherwood number and an increase in the Nusselt number.

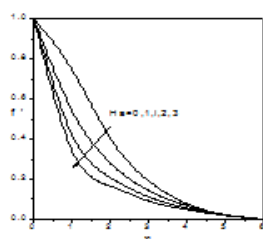


Fig.1: Variation of the velocity  $f'$  with  $Ha$  for  $Pr=0.71$ ,  $Sc=0.24$ ,  $Gr=Gc=Ec=1$ ,  $Du=0.2$ ,  $Sr=\beta=0.1$ .

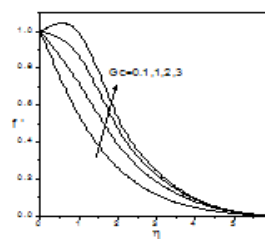


Fig.3: Variation of the velocity  $f'$  with  $Gc$  for  $Pr=0.71$ ,  $Sc=0.24$ ,  $Gr=Ec=1$ ,  $Du=0.2$ ,  $Sr=Ha=\beta=0.1$ .

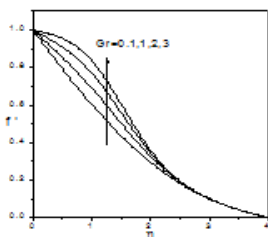


Fig.2: Variation of the velocity  $f'$  with  $Gr$  for  $Pr=0.71$ ,  $Sc=0.24$ ,  $Gc=Ec=1$ ,  $Du=0.2$ ,  $Sr=Ha=\beta=0.1$ .

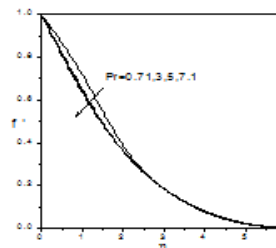


Fig.4: Variation of the velocity  $f'$  with  $Pr$  for  $Sc=0.62$ ,  $Gr=Gc=Ec=1$ ,  $Du=0.2$ ,  $Sr=Ha=\beta=0.1$ .

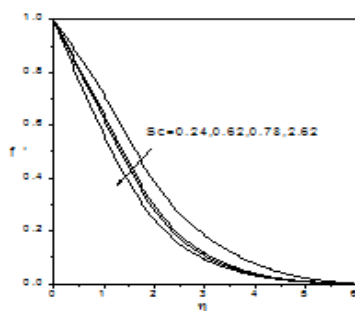


Fig.5: Variation of the velocity  $f'$  with  $Sc$  for  $Pr=0.71$ ,  $Gr=Gc=Ec=1$ ,  $Du=0.2$ ,  $Sr=Ha=\beta=0.1$ .

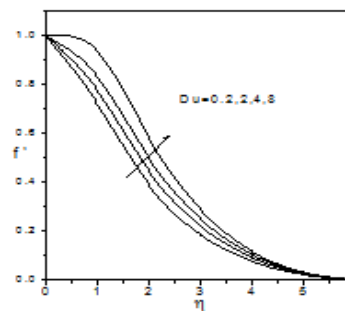


Fig.8: Variation of the velocity  $f'$  with  $Du$  for  $Pr=0.71$ ,  $Sc=0.24$ ,  $Gr=Gc=Ec=1$ ,  $Sr=Ha=\beta=0.1$ .

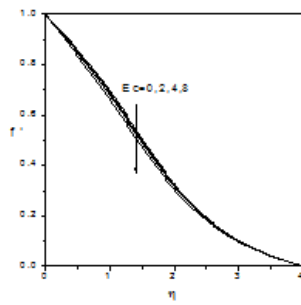


Fig.6: Variation of the velocity  $f'$  with  $Ec$  for  $Pr=0.71$ ,  $Sc=0.24$ ,  $Gr=Gc=1$ ,  $Du=0.2$ ,  $Sr=Ha=\beta=0.1$ .

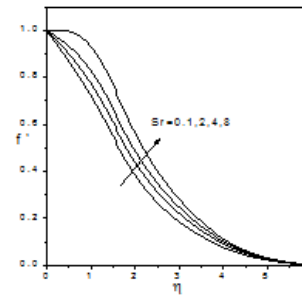


Fig.9: Variation of the velocity  $f'$  with  $Sr$  for  $Pr=0.71$ ,  $Sc=0.24$ ,  $Gr=Gc=Ec=1$ ,  $Du=0.2$ ,  $Ha=\beta=0.1$ .

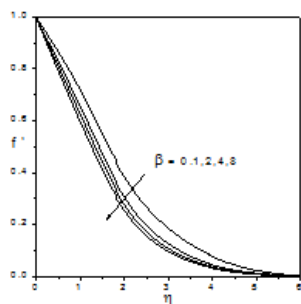


Fig.7: Variation of the velocity  $f'$  with  $\beta$  for  $Pr=0.71$ ,  $Sc=0.24$ ,  $Gr=Gc=Ec=1$ ,  $Du=0.2$ ,  $Sr=Ha=0.1$ .

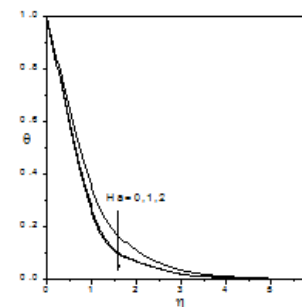


Fig.10: Variation of the temperature  $\theta$  with  $Ha$  for  $Pr=0.71$ ,  $Sc=0.24$ ,  $Gc=Gr=Ec=1$ ,  $Du=0.2$ ,  $Sr=\beta=0.1$ .

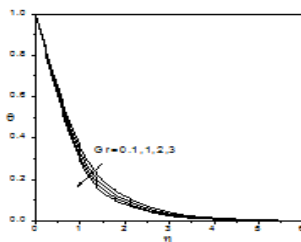


Fig. 11: Variation of the temperature  $\theta$  with  $Gr$  for  $Pr=0.71$ ,  $Sc=0.24$ ,  $Gc=Ec=1$ ,  $Du=0.2$ ,  $Sr=Ha=\beta=0.1$ .

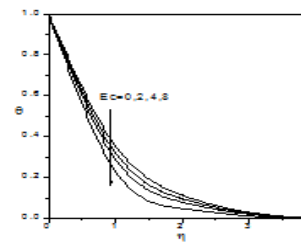


Fig.14: Variation of the temperature  $\theta$  with  $Ec$  for  $Pr=0.71$ ,  $Sc=0.24$ ,  $Gr=Gc=1$ ,  $Du=0.2$ ,  $Sr=Ha=\beta=0.1$ .

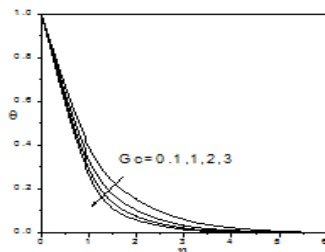


Fig.12: Variation of the temperature  $\theta$  with  $Gc$  for  $Pr=0.71$ ,  $Sc=0.24$ ,  $Gr=Ec=1$ ,  $Du=0.2$ ,  $Sr=Ha=\beta=0.1$ .

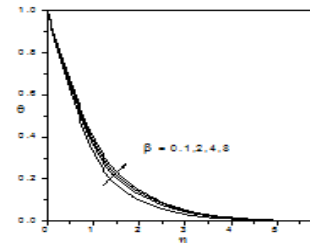


Fig.15: Variation of the temperature  $\theta$  with  $\beta$  for  $Pr=0.71$ ,  $Sc=0.24$ ,  $Gr=Ec=Gc=1$ ,  $Du=0.2$ ,  $Sr=Ha=0.1$ .

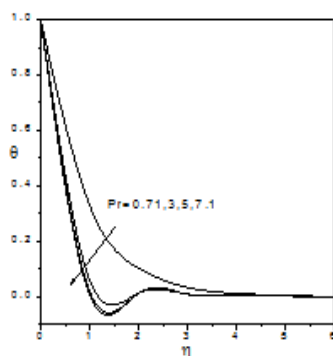


Fig.13: Variation of the temperature  $\theta$  with  $Pr$  for  $Sc=0.24$ ,  $Gr=Ec=Gc=1$ ,  $Du=0.2$ ,  $Sr=Ha= \beta=0.1$ .

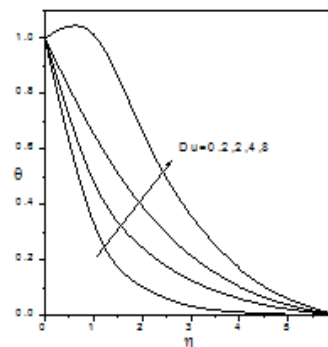


Fig.16: Variation of the temperature  $\theta$  with  $Du$  for  $Pr=0.71$ ,  $Sc=0.24$ ,  $Gr=Ec=Gc=1$ ,  $Sr= \beta=Ha=0.1$ .

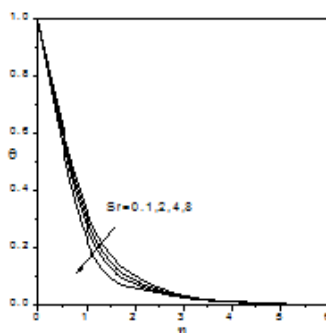


Fig.17: Variation of the temperature  $\theta$  with  $Sr$  for  $Pr=0.71$ ,  $Sc=0.24$ ,  $Gr=Ec=Gc=1$ ,  $Du=0.2$ ,  $Sr=Ha= \beta=0.1$ .

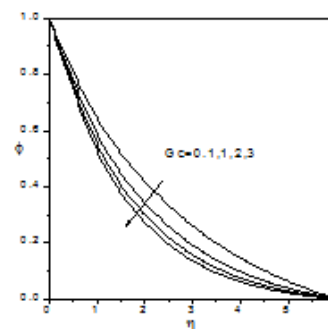


Fig.20: Variation of the concentration  $\phi$  with  $Gc$  for  $Pr=0.71$ ,  $Sc=0.24$ ,  $Gr=Ec=1$ ,  $Du=0.2$ ,  $Sr=Ha= \beta=0.1$ .

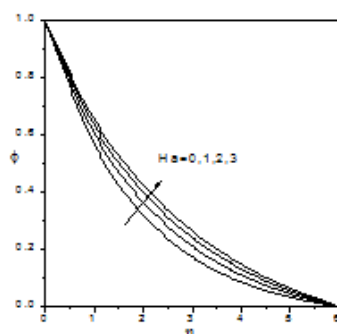


Fig.18: Variation of the concentration  $\phi$  with  $Ha$  for  $Pr=0.71$ ,  $Sc=0.24$ ,  $Gc=Gr=Ec=1$ ,  $Du=0.2$ ,  $Sr= \beta=0.1$ .

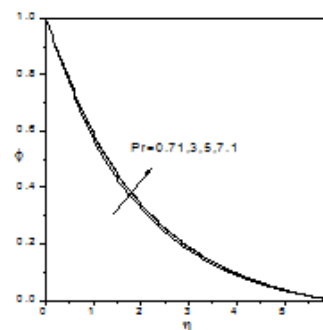


Fig.21: Variation of the concentration  $\phi$  with  $Pr$  for  $Sc=0.24$ ,  $Gr=Gc=Ec=1$ ,  $Du=0.2$ ,  $Sr=Ha= \beta=0.1$ .

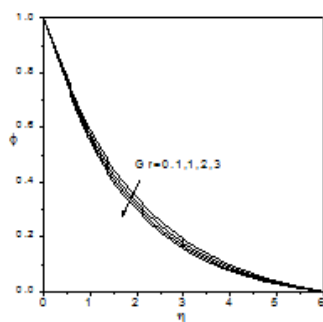


Fig.19: Variation of the concentration  $\phi$  with  $Gr$  for  $Pr=0.71$ ,  $Sc=0.24$ ,  $Gc=Ec=0.1$ ,  $Du=0.2$ ,  $Sr=Ha= \beta=0.1$ .

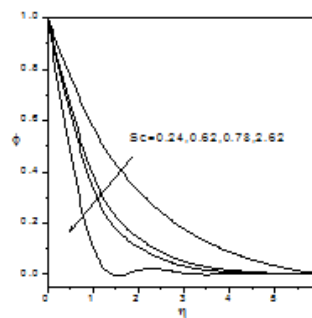


Fig.22: Variation of the concentration  $\phi$  with  $Sc$  for  $Pr=0.71$ ,  $Gr=Gc=Ec=1$ ,  $Du=0.2$ ,  $Sr=Ha= \beta=0.1$ .

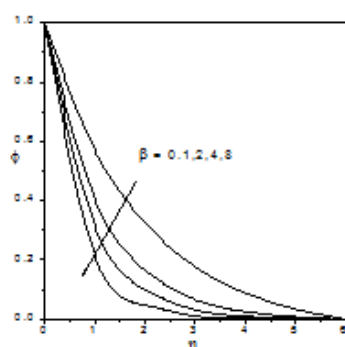


Fig.23: Variation of the concentration  $\phi$  with  $\beta$  for  $Pr=0.71$ ,  $Sc=0.24$ ,  $Gr=Gc=Ec=1$ ,  $Du=0.2$ ,  $Sr=Ha=0.1$ .

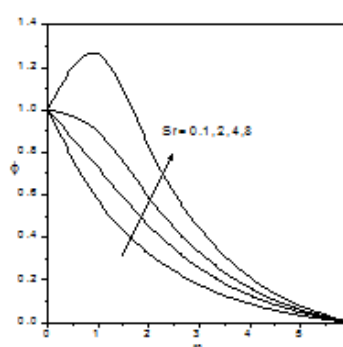


Fig.25: Variation of the concentration  $\phi$  with  $Sr$  for  $Pr=0.71$ ,  $Sc=0.24$ ,  $Gr=Gc=Ec=1$ ,  $Du=0.2$ ,  $Ha= \beta=0.1$ .

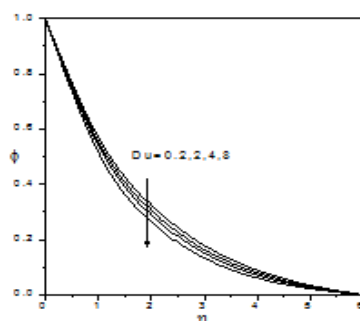


Fig.24: Variation of the concentration  $\phi$  with  $Du$  for  $Pr=0.71$ ,  $Sc=0.24$ ,  $Gr=Gc=Ec=0.1$ ,  $Sr= \beta=Ha=0.1$ .

**Table 1** Comparison of the present results with Ibrahim and Makinde [9]  
 for  $f''(0), -\theta'(0), -\phi'(0)$  when  $Du=Sr=0$  for  $Sc=0.24$ .

Ha	Gr	Gc	Pr	Ec	$\beta$	Ibrahim and Makinde[9]			Present work		
						$f''(0)$	$-\theta'(0)$	$-\phi'(0)$	$f''(0)$	$-\theta'(0)$	$-\phi'(0)$
0.0	0.1	0.1	0.71	0.1	0.1	-0.8672315153	0.845372426	0.4538848758	-0.86894	0.844087	0.456754
1.0	0.1	0.1	0.71	0.1	0.1	-1.3040411834	0.769606228	0.3968458010	-1.30465	0.769761	0.403069
2.0	0.1	0.1	0.71	0.1	0.1	-1.6363224533	0.7152561700	0.3637592785	-1.63769	0.723342	0.390404
3.0	0.1	0.1	0.71	0.1	0.1	-1.914170216	0.6748301664	0.3417321548	-1.91829	0.72123	0.385598
0.1	1.0	0.1	0.71	0.1	0.1	-0.3839658694	0.95276174188	0.5268684571	-0.506723	0.909116	0.501291
0.1	2.0	0.1	0.71	0.1	0.1	0.11763577749	1.02373066746	0.5739990411	-0.0984307	0.963598	0.531531
0.1	3.0	0.1	0.71	0.1	0.1	0.57540541047	1.07621858633	0.6081067643	0.278976	1.00562	0.554932
0.1	0.1	1.0	0.71	0.1	0.1	-0.5036924009	0.91055575959	0.4901999207	-0.393603	0.948007	0.529538
0.1	0.1	2.0	0.71	0.1	0.1	-0.0963335838	0.96454281127	0.521869527	0.108696	1.02014	0.574809
0.1	0.1	3.0	0.71	0.1	0.1	0.28056792190	1.0063088977	0.5462127475	0.567359	1.07338	0.608279
0.1	0.1	0.1	1.0	0.1	0.1	-0.9249676483	1.03144243794	0.4442962139	-0.929989	1.028	0.458367
0.1	0.1	0.1	5.0	0.1	0.1	-0.9469422732	2.5856233329	0.4402201913	-0.952349	2.58349	0.454493
0.1	0.1	0.1	7.1	0.1	0.1	-0.9502609122	3.1264076966	0.4399339618	-0.955687	3.12442	0.454213
0.1	0.1	0.1	0.71	1.0	0.1	-0.9514562137	3.282065838	0.4397836153	-0.924247	0.860469	0.460006
0.1	0.1	0.1	0.71	2.0	0.1	-0.9527820463	3.4548206835	0.43961672419	-0.924864	0.889753	0.459863
0.1	0.1	0.1	0.71	3.0	0.1	-0.9541054829	3.62736701503	0.43945000226	-0.925479	0.918994	0.459721
0.1	0.1	0.1	0.71	0.1	1.0	-0.9664432051	3.1207006382	0.66834955297	-0.934717	0.827817	0.673372
0.1	0.1	0.1	0.71	0.1	3.0	-0.9791178642	3.1163155824	0.97930723624	-0.945602	0.822187	0.981507

**Table 2** Numerical values of  $f''(0), -\theta'(0), -\phi'(0)$   
 for  $Gr = Gc = Ec = 1, Pr = 0.71, \beta = Ha = 0.1$  when  $Sc = 0.24$ .

Du	Sr	$f''(0)$	$-\theta'(0)$	$-\phi'(0)$
0.2	0.1	-0.0318096	1.00205	0.53702
2.0	0.1	0.042471	0.712256	0.55754
4.0	0.1	0.122937	0.370637	0.578394
8.0	0.1	0.280291	-0.377716	0.616786
0.2	1.0	0.00233155	1.02791	0.390312
0.2	2.0	0.040576	1.05695	0.217629
0.2	3.0	0.0791798	1.08652	0.0341978

**REFERENCES**

[1]. Nield D.A. and Bejan A. (1999), Convection in Porous Media, 2nd Ed, Springer, N.Y.  
 [2]. Ingham D.B. and Pop I. (1998), Transport Phenomena in Porous Media, I, Pergamon, Oxford.  
 [3]. Ingham D.B. and Pop I. (2002), Transport Phenomena in Porous Media II, Pergamon, Oxford.  
 [4]. Bejan A. and Khair K.R. (1985), Heat and mass transfer by natural convection in a porous medium, Int. J. Heat Mass Trans., Vol.28, pp.909-918.  
 [5]. Trevisan O.V. and Bejan A. (1990), Combined heat and mass transfer by natural convection in a porous medium, Adv. Heat Trans., Vol.20, pp.315-352.  
 [6]. Sakiadis B.C. (1961), Boundary layer behavior on continuous solid surface for two dimensional and axisymmetric flow, AIChE. J., Vol. 7, pp.26-28.  
 [7]. Postelnicu A. (2004), Influence of magnetic field on heat and mass transfer by natural convection from vertical surfaces in porous media considering Soret and Dufour effects, Int. J. Heat Mass Trans., Vol.47, pp.14670-1472.  
 [8]. Alam M.S. and Rahman M.M. (2006), Dufour and Soret Effects on Mixed Convection Flow past a Vertical Porous Flat Plate with Variable Suction, Nonlinear Analysis, Model. Control., Vol.11(1), pp. 3-12.  
 [9]. Anghel M., Takhar H.S. and Pop I. (2000), Dufour and Soret effects on free convection boundary layer over a vertical surface embedded in a porous medium, Studia Universitatis Babeş- Bolyai, Mathematica, Vol.45(4), pp.11-21.  
 [10]. Chang C. and Lee Z. (2008), Free convection on a vertical plate with uniform and constant heat flux in a thermally stratified micropolar fluid, Mech. Res. Comm., Vol. 35, pp.421-427  
 [11]. Vajravelu K. and Nayfeh J. (1993), Convective heat transfer at a stretching sheet, Acta Mechanica, Vol.96, pp.47-54.  
 [12]. Crane L.J. (1970), Flow past a stretching sheet, ZAMP, Vol.21, pp.645-647.

- [13]. Gupta P.S. and Gupta A.S. (1977), Heat and Mass Transfer on a stretching sheet with suction or blowing, *Canda. J. Chem. Eng.*, Vol.55, pp.744-746.
- [14]. Kays W.M. and Crawford M.E. (1993), *Convective heat and mass transfer*, McGraw-Hill.
- [15]. Ibrahim S.Y. and Makinde O.D.(2010a), On MHD boundary layer flow of chemically reacting fluid with heat and mass transfer past a stretching sheet, *Int. J. Fluid Mech.*, Vol.2(2), pp.123-132.
- [16]. Ibrahim S.Y. and Makinde O.D. (2010b), Chemically reacting MHD boundary layer flow of heat and mass transfer over a moving vertical plate with suction, *Sci. Res. and Essays.*, Vol.5(19), pp.2875-2882.
- [17]. Anwar Bég O., Joaquín Z. and Takhar H.S. (2008), Laminar free convection from a continuously-moving vertical surface in thermally-stratified non-Darcian high-porosity medium, Network numerical study, *Int. Commun. Heat Mass Trans.*, Vol.35, pp.810-816.
- [18]. pp.810-816.
- [19]. Makinde O.D. (2005), Free-convection flow with thermal radiation and mass transfer past a moving vertical porous plate, *Int. Comm. Heat Mass Trans.*, Vol.32, pp.1411-1419.
- [20]. Makinde O.D. and Ogulu A. (2008), The effect of thermal radiation on the heat and mass transfer flow of a variable viscosity fluid past vertical porous plate permeated by transverse magnetic field, *Chem. Eng. Comm.*, Vol.195(12), pp.1575-1584.
- [21]. Gebhart B. (1962), Effects of viscous dissipation in natural convection, *J.Fluid Mechanics.*, Vol.14, pp.225-232.
- [22]. Gebhart B. and Mollendorf J. (1969), Viscous dissipation in external natural convection flows., *J. Fluid .Mech.*,Vol. 38, pp.97-107.
- [23]. Soundalgekar V.M. (1972), Viscous Dissipation effects on unsteady free convective flow past an infinite, vertical porous plate with constant suction, *Int. J. Heat Mass Transfer*, Vol.15, pp.253-1261.
- [24]. Israel-Cookey C., Ogulu A., and Omubo-Pepple V.M. (2003), Influence of viscous dissipation on unsteady MHD free convection flow past an infinite vertical plate in porous medium with time-dependent suction, *Int. J. Heat Mass Transfer*, Vol.46, pp. 2305-2311.
- [25]. pp. 2305-2311.
- [26]. Soundalgekar V.M and Hiremath S.V. (1983), Finite difference analysis of mass transfer effects on flow past an impulsively started infinite isothermal vertical plate in dissipative fluid, *Astro Physics and Space Science*, Vol.95, pp.163-173.

International Journal of Engineering Research and Applications (IJERA) is **UGC approved** Journal with Sl. No. 4525, Journal no. 47088. Indexed in Cross Ref, Index Copernicus (ICV 80.82), NASA, Ads, Researcher Id Thomson Reuters, DOAJ.

E. Manjoolatha . “Soret And Dufour Effects On Mhd Boundary Layer Flow Of A Chemically Reacting Fluid Past A Movng Vertical Plate With Viscous Dissipation.” *International Journal of Engineering Research and Applications (IJERA)* , vol. 7, no. 9, 2017, pp. 80–89.